

# Rate equations for nitrogen molecules in ultrashort and intense x-ray pulses‡

Ji-Cai Liu (刘纪彩),<sup>1,2</sup> Nora Berrah,<sup>3</sup> Lorenz S. Cederbaum,<sup>4</sup>  
James P. Cryan,<sup>5,6</sup> James M. Glowia,<sup>5,6</sup> Kenneth J. Schafer,<sup>5,7</sup>  
and Christian Buth<sup>2,4,5,7</sup>

<sup>1</sup> Department of Mathematics and Physics, North China Electric Power University, 102206 Beijing, China

<sup>2</sup> Max-Planck-Institut für Kernphysik, Saupfercheckweg 1, 69117 Heidelberg, Germany

<sup>3</sup> Department of Physics, University of Connecticut, 2152 Hillside Road, U-3046, Storrs, Connecticut 06269, USA

<sup>4</sup> Theoretische Chemie, Physikalisch-Chemisches Institut, Im Neuenheimer Feld 229, Ruprecht-Karls-Universität Heidelberg, 69120 Heidelberg, Germany

<sup>5</sup> The PULSE Institute for Ultrafast Energy Science, SLAC National Accelerator Laboratory, Menlo Park, California 94025, USA

<sup>6</sup> Department of Physics, Stanford University, Stanford, California 94305, USA

<sup>7</sup> Department of Physics and Astronomy, Louisiana State University, Baton Rouge, Louisiana 70803, USA

E-mail: christian.buth@web.de, World Wide Web: [www.christianbuth.name](http://www.christianbuth.name)

**Abstract.** We study theoretically the quantum dynamics of nitrogen molecules ( $N_2$ ) exposed to intense and ultrafast x-rays at a wavelength of 1.1 nm (1100 eV photon energy) from the Linac Coherent Light Source (LCLS) free electron laser. Molecular rate equations are derived to describe the intertwined photoionization, decay, and dissociation processes occurring for  $N_2$ . This model complements our earlier phenomenological approaches, the single-atom, symmetric-sharing, and fragmentation-matrix models of J. Chem. Phys. **136**, 214310 (2012). Our rate-equations are used to obtain the effective pulse energy at the sample and the time scale for the dissociation of the metastable dication  $N_2^{2+}$ . This leads to a very good agreement between the theoretically and experimentally determined ion yields and, consequently, the average charge states. The effective pulse energy is found to decrease with shortening pulse duration. This variation together with a change in the molecular fragmentation pattern and frustrated absorption—an effect that reduces absorption of x-rays due to (double) core hole formation—are the causes for the drop of the average charge state with shortening LCLS pulse duration discovered previously.

PACS numbers: 33.80.-b, 33.80.Eh, 32.80.Aa, 41.60.Cr

‡ This is an author-created, un-copyedited version of an article accepted for publication in Journal of Physics B: Atomic, Molecular and Optical Physics. IOP Publishing Ltd is not responsible for any errors or omissions in this version of the manuscript or any version derived from it. The Version of Record is available online at [doi:10.1088/0953-4075/49/7/075602](https://doi.org/10.1088/0953-4075/49/7/075602).

*Keywords:* nitrogen molecule, molecular rate equations, frustrated absorption, ultrafast, intense, x-rays, fragmentation

*Date:* 16 March 2017

## 1. Introduction

With the development of x-ray lasers, especially the state-of-the-art x-ray free electron lasers (FELs), the exploration of the interaction of intense and ultrafast x-rays with matter has become a scientific frontier [1–18]. The extreme pulse characteristics of operational x-ray FELs—such as the the Linac Coherent Light Source (LCLS) [19, 20] in Menlo Park, California, USA—are ultrahigh brightness, femtosecond pulse duration, short wavelengths, and transverse coherence. The novel properties of x-rays enable the study of ultrafast multiphoton interaction of x-rays with matter and spawned the subfield of x-ray quantum optics [21]. Specifically, the intense x-rays from FELs induce two-photon absorption [22] (extreme ultraviolet (XUV) [23]), Rabi flopping [24, 25], photoelectron holography [26], single-pulse pump-probe experiments [27], stimulated x-ray Raman scattering [28], and four-wave mixing [28] (XUV [29]), suppress the branching ratio of Auger decay [30] or produce interference effects in Auger decay [31, 32]. Saturable [33] and frustrated absorption [1, 4, 34] (XUV [35]) reduce radiation damage of the sample and may thus be beneficial for diffraction experiments at FELs [36]. The combination of intense and ultrafast x-rays with an optical laser offers perspectives for the control of x-ray lasing [37], high-order harmonic generation in the kiloelectronvolt regime [38–41], and the production of high-energy frequency combs [42, 43].

Initially, atoms were studied in intense and ultrafast soft x-ray pulses from LCLS [4]. Neon was chosen as a prototypical atom [4] and it was found that, for sufficiently high photon energies, all atomic electrons are ionized by one-x-ray-photon absorption and atoms even become transparent at high x-ray intensity due to rapid ejection of inner-shell electrons. Ionization by x-rays [4] (XUV [44, 45]) progresses *from the inside out* in contrast to strong-field ionization with intense optical lasers where ionization of the outermost electrons occurs, i.e., there ionization proceeds *from the outside in*. The quantum dynamics of neon atoms in intense and ultrashort x-ray radiation was successfully described theoretically with a rate-equation model [4, 46] foreshadowing extension to more complex systems.

Understanding the response of molecules to intense and ultrafast x-rays poses substantial complications over the description of atoms [1–3, 27, 34, 47]; namely, in addition to photoionization and intraatomic decay processes, for molecules, there are also molecular fragmentation, and sharing of the charges in the valence shells among the nuclei which need to be regarded. The quantum dynamics induced in molecules by soft x-rays [1–3, 27, 34, 47] from FELs (XUV [48–50]), has been studied in experiments during the last few years. The first ever study of a molecule, namely nitrogen ( $\text{N}_2$ ), in intense and ultrafast x-rays was performed at LCLS [1] where  $\text{N}_2$  was chosen because it is an important but simple molecule. The experiment used x-rays with a wavelength

of 1.1 nm, i.e., 1100 eV photon energy. We found [1] that the absorption of x-rays is frustrated, i.e., pulses with a comparable energy but decreasing duration lead to smaller average charge states compared with longer pulses and thus a reduced absorption of x-rays. Unlike the XUV photon energy regime in which multiphoton absorption causes single or multiple ionization [48–50], predominantly only one-photon ionization occurs in the x-ray regime [1, 4, 27, 34] which is a substantial simplification of the problem.

To find a theoretical description of  $N_2$  in intense and ultrafast x-rays, we devised a series of phenomenological models of increasing sophistication, namely, a single-atom model, a symmetric-sharing model, and a fragmentation-matrix model [34]. It was found that a single-atom model—which assumes that the molecular ion yields are the same as the ion yields that are obtained from a single atom—is not capable to describe the experimental data for  $N_2$  due to a redistribution of valence charges over both N atoms in the molecule after ionization and prior breakup. Therefore, a symmetric-sharing model was tried next in which the molecular charge is distributed evenly between the two atoms. The model was found to lead to a similarly deficient description as the single-atom model. Thus the insights gained from these two models were used to devise heuristically a fragmentation-matrix model in which there is only a partial redistribution of charges between the two atoms. This model clearly reveals the relevance of the redistribution of charge and a different weighting of electronic processes and nuclear dynamics on short and long time scales for similar nominal pulse energy but varying pulse duration.

In this article, we study sequential multiple ionization of  $N_2$  induced by intense and ultrafast x-rays from LCLS with comparable nominal pulse energy but different pulse durations. In the theory section 2, we extend our modeling from [34] by devising a molecular rate-equation formalism§ to describe the quantum dynamics induced by x-ray absorption. The molecular rate equations are formulated for neutral  $N_2$  and molecular cations with single core holes (SCHs), double core holes (DCHs) on a single site (ssDCH), and double core holes on two sites (tsDCH) [10, 34, 51–53]. Further rate equations for valence ionized molecular configurations and even triple core holes round off the set. In total, we consider all possible one-photon absorption and Auger decay channels for molecular charge states up to  $N_2^{3+}$  [34, 54]. We treat molecular charge states beyond  $N_2^{3+}$  as fragmented into single atoms and we take all single atom charge states into account in terms of atomic rate equations [34, 54]. By considering the finite lifetime of the metastable molecular dication  $N_2^{2+}$  and the sharing of the valence electrons between the two nuclei of the molecule, the experimental ion yields and the average charge state are well reproduced in the results and discussion section 3. Our present molecular rate-equation model shows that the differences in the ion yields observed for pulses of varying durations are due to the competition between photoabsorption, Auger

§ The model for  $N_2$  in intense and ultrafast x-rays of Ref. [1] is also based on molecular rate equations and was developed by Oleg Kornilov and Oliver Gessner. The rate equations in this work were devised independently and their results are consistent with the phenomenological models of [34] and further analysis of the experimental data in [27] unlike the previous attempt in Ref. [1].

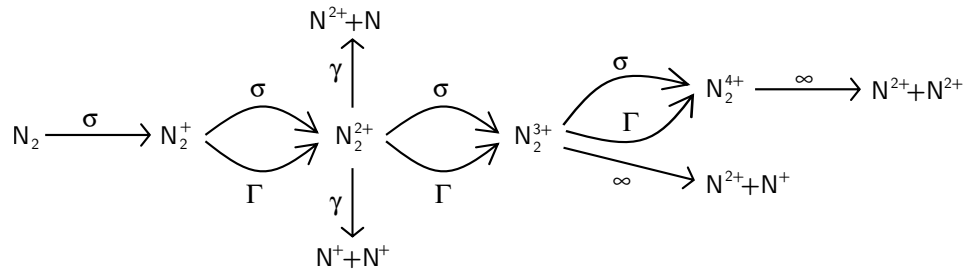


**Figure 1.** Schematic of the interaction of  $N_2$  with intense x-rays. The molecular processes displayed are photoionization by one-x-ray-absorption “ $\sigma$ ”, Auger decay of core-ionized states “ $\Gamma$ ”, dissociation of the metastable molecular ions  $N_2^{2+}$  with a fragmentation rate “ $\gamma$ ”, and instantaneous fragmentation “ $\infty$ ”. In the last step of the interaction “ $\infty$ ” occurs, if no core holes are present in  $N_2^{3+}$ ; otherwise “ $\sigma$ ” or “ $\Gamma$ ” take place.

decay processes, and molecular fragmentation. Frustrated absorption is explained as a reduction of photoabsorption by core hole formation. The effective pulse energy at the sample and the rate of the dissociation of the molecular dication are obtained with the molecular rate-equation model by comparing theoretical and experimental data. Our rate-equation model represents an improvement over the fragmentation-matrix model [34] as it describes the quantum dynamics of the involved molecular charge states and the breakup process. Nonetheless, the results from our model agree well with our earlier findings [34]. Conclusions are drawn in section 4. All details of the molecular rate-equation model and the calculations in this article are provided in the Supplementary Data [54].

Atomic units [56, 57] are used throughout unless stated otherwise. For the conversion of a decay width  $\Gamma$  in electronvolts to a lifetime  $\tau$  in femtoseconds, we use the relation  $\tau = \frac{\hbar}{\Gamma} = \frac{0.658212 \text{ eV fs}}{\Gamma}$ .

## 2. Theory

We develop a rate-equation description for  $N_2$  in intense and ultrafast x-rays which includes the molecular processes schematically depicted in figure 1. Initially, all  $N_2$  molecules are in their ground state. The absorption of an x ray creates the molecular cation  $N_2^+$  which is frequently metastable with respect to dissociation. Thus  $N_2^+$  remains a molecule until either another x ray is absorbed or, if there is a core hole, Auger decay takes place [58–61]. Both processes promote  $N_2^+$  to the dication  $N_2^{2+}$ . Even  $N_2^{2+}$  that, in our case, is predominantly produced by Auger decay, is frequently metastable with a comparatively long lifetime of  $\sim 100$  fs with respect to dissociation [62, 63]. There are three channels for  $N_2^{2+}$  to evolve into; first,  $N_2^{2+}$  fragments causing the end of the molecule; second, an x ray is absorbed, and, third, if there is a core hole, Auger decay occurs. Both the second and the third channel promote  $N_2^{2+}$  to  $N_2^{3+}$ . If  $N_2^{3+}$  has no core holes, we assume that it fragments immediately into atoms; otherwise, again x-ray absorption and Auger decay may occur turning  $N_2^{3+}$  into  $N_2^{4+}$  which is

considered to fragment immediately into two  $\text{N}^{2+}$  atoms [64, 65]. From here onwards, only atomic fragments are considered and their further evolution is governed by atomic rate equations.

Molecular rate equations are formulated for  $\text{N}_2$  incorporating the steps mentioned in the previous paragraph. Altogether there are thirty-three molecular configurations from neutral  $\text{N}_2$  to triply charged  $\text{N}_2^{3+}$  with different combinations of the electronic configurations of the two atomic sites. The quantum dynamics of the atomic fragments after breakup is described with an atomic rate-equation model which is modified in order to funnel probability from the molecular rate equations into the atomic rate equations. All in all, we extend nine of the thirty-six atomic rate equations to describe the transfer of probability from molecular configurations to atomic configurations. The molecular and atomic rate equations incorporate all energetically accessible atomic one-photon absorption processes together with fluorescence and Auger decay of multiply-charged nitrogen atoms [34]; simultaneous multiphoton absorption [22, 46, 66] and multielectron processes such as shake off [22] and double Auger decay [67], however, are neglected. In what follows, we write down selected molecular rate equations to show the guiding principles. The complete set of equations is provided in the Supplementary Data [54].

### 2.1. Neutral nitrogen molecule $\text{N}_2$

We specify probabilities  $\tilde{P}_{ijk,\ell mn}(t)$  at time  $t$  for  $0 \leq i, j, \ell, m \leq 2 \wedge 0 \leq k, n \leq 3$  to find an  $\text{N}_2$  molecule in which the individual N atoms have the electronic configurations  $1s^i 2s^j 2p^k$  and  $1s^\ell 2s^m 2p^n$ , respectively, which are abbreviated by  $\{ijk\}$  and  $\{\ell mn\}$ . Molecular configurations for  $\text{N}_2$  are written succinctly as  $\{ijk, \ell mn\}||$ . X-ray absorption by  $\text{N}_2$  is governed by a single rate equation:

$$\frac{d\tilde{P}_{223,223}(t)}{dt} = -2 \sigma_{223} \tilde{P}_{223,223}(t) J_X(t) , \quad (1)$$

with the total one-x-ray-photon absorption cross section  $\sigma_{ijk}$  of an N atom in configuration  $\{ijk\}$  where  $i = 2, j = 2, k = 3$  denotes the neutral N atom in the ground state. The factor of 2 accounts for the two atoms in  $\text{N}_2$  and the minus sign indicates a depletion of  $\text{N}_2$  in the ground state by x-ray absorption. Further,  $J_X(t)$  is the x-ray photon flux at time  $t$ . Note that the x-ray flux has, in principle, both temporal and spatial dependence due to the longitudinal and transverse profiles of the x-ray beam [34]. For simplicity of notation, we do not explicitly write spatial coordinates for the quantities involved but state all equations for a flux that depends only on time  $J_X(t)$ .

### 2.2. Molecular nitrogen cation $\text{N}_2^+$

For the singly-charged molecule  $\text{N}_2^+$  with a SCH, the governing rate equation reads

$$\frac{d\tilde{P}_{123,223}(t)}{dt} = 2 \sigma_{123\leftarrow 223} \tilde{P}_{223,223}(t) J_X(t) \quad (2)$$

|| Note that  $\{ijk, \ell mn\} = \{\ell mn, ijk\}$  holds, i.e., only distinct molecular configurations up to a permutation are considered to avoid double counting.

$$- (\sigma_{123} + \sigma_{223}) \tilde{P}_{123,223}(t) J_X(t) - \Gamma_{123} \tilde{P}_{123,223}(t) ,$$

where  $\sigma_{\ell mn \leftarrow ijk}$  stands for the one-x-ray-photon absorption cross section which causes an N atom with the configuration  $\{ijk\}$  to transition into the configuration  $\{\ell mn\}$ . With  $\Gamma_{ijk}$  we denote the total decay rate of an N atom in configuration  $\{ijk\}$  to any final state. The first term on the right-hand side of (2) is the rate of production of  $\{123, 223\}$  by x-ray absorption; the second term describes the rate of depletion by x-ray absorption; and the third term represents the rate of decay.

Further molecular rate equations are formulated for the other cationic configurations of  $N_2^+$  which are  $\{213, 223\}$  and  $\{222, 223\}$ ; the resulting molecular rate equations are expressed analogously to (2) [54]. Only few nondissociated  $N_2^+$  molecules were detected in the experiment [1] which justifies that we do not treat them as a channel but break them into atomic fragments at  $t \rightarrow \infty$ .

### 2.3. Molecular nitrogen dication $N_2^{2+}$

For the molecular dication  $N_2^{2+}$  with only valence vacancies, we have the exemplary rate equation

$$\begin{aligned} \frac{d\tilde{P}_{212,223}(t)}{dt} = & \sigma_{212 \leftarrow 213} \tilde{P}_{213,223}(t) J_X(t) + \sigma_{212 \leftarrow 222} \tilde{P}_{222,223}(t) J_X(t) \quad (3) \\ & - (\sigma_{212} + \sigma_{223}) \tilde{P}_{212,223}(t) J_X(t) + \Gamma_{212 \leftarrow 123} \tilde{P}_{123,223}(t) \\ & - \gamma \tilde{P}_{212,223}(t) , \end{aligned}$$

where  $\Gamma_{\ell mn \leftarrow ijk}$  is the decay rate of the atom in configuration  $\{ijk\}$  into  $\{\ell mn\}$ . The fragmentation rate of the valence-ionized molecular dication  $N_2^{2+}$  is indicated by  $\gamma$  which is presumed not to depend on the molecular configuration. We assume that all  $N_2^{2+}$  eventually dissociate because only few nondissociated  $N_2^{2+}$  molecules were detected in the experiment [1].

Since  $N_2^{2+}$  dissociates either symmetrically into  $N^+ + N^+$  or asymmetrically into  $N + N^{2+}$ , the parameters  $f_{N^++N^+}$  and  $f_{N+N^{2+}}$  are introduced [34] to account for the probabilities to dissociate into the fragmentation channels



with  $f_{N^++N^+} + f_{N+N^{2+}} = 1$ . The molecular probability of  $N_2^{2+}$  upon breakup needs to be funneled into the atomic rate equations. For example, the atomic rate equation of a neutral N atom has to be modified to

$$\begin{aligned} \frac{dP_{223}(t)}{dt} = & - \sigma_{223} P_{223}(t) J_X(t) \\ & + f_{N+N^{2+}} \frac{\gamma}{2} \left[ \tilde{P}_{203,223}(t) + \tilde{P}_{212,223}(t) + \tilde{P}_{221,223}(t) \right. \\ & \left. + \tilde{P}_{213,213}(t) + \tilde{P}_{213,222}(t) + \tilde{P}_{222,222}(t) \right] , \quad (5) \end{aligned}$$

where  $P_{lmn}(t)$  is the probability to find an N atom at time  $t$  in electronic configuration  $\{lmn\}$ . The last term on the right-hand side of (5) is new compared with the original atomic rate equation and it is responsible for funneling probability of neutral N atoms due to molecular fragmentation from the molecular configurations  $\{203, 223\}$ ,  $\{212, 223\}$ ,  $\{221, 223\}$ ,  $\{213, 213\}$ ,  $\{213, 222\}$ , and  $\{222, 222\}$ . Similar modifications are made to the atomic rate equations for the configurations  $\{213\}$ ,  $\{222\}$ ,  $\{203\}$ ,  $\{212\}$ ,  $\{221\}$ ,  $\{113\}$ ,  $\{122\}$ , and  $\{023\}$  [54]. Other atomic rate equations are not altered.

For a valence hole and a SCH on one atom, the dynamics is quantified by the molecular rate equation

$$\begin{aligned} \frac{d\tilde{P}_{113,223}(t)}{dt} = & \sigma_{113\leftarrow 213} \tilde{P}_{213,223}(t) J_X(t) + \sigma_{113\leftarrow 123} \tilde{P}_{123,223}(t) J_X(t) \quad (6) \\ & - (\sigma_{113} + \sigma_{223}) \tilde{P}_{113,223}(t) J_X(t) - \Gamma_{113} \tilde{P}_{113,223}(t) , \end{aligned}$$

for a tsDCH by

$$\begin{aligned} \frac{d\tilde{P}_{123,123}(t)}{dt} = & \sigma_{123\leftarrow 223} \tilde{P}_{123,223}(t) J_X(t) - 2 \sigma_{123} \tilde{P}_{123,123}(t) J_X(t) \quad (7) \\ & - 2 \Gamma_{123} \tilde{P}_{123,123}(t) , \end{aligned}$$

and for a ssDCH by

$$\begin{aligned} \frac{d\tilde{P}_{023,223}(t)}{dt} = & \sigma_{023\leftarrow 123} \tilde{P}_{123,223}(t) J_X(t) - (\sigma_{023} + \sigma_{223}) \tilde{P}_{023,223}(t) J_X(t) \quad (8) \\ & - \Gamma_{023} \tilde{P}_{023,223}(t) . \end{aligned}$$

We see from these expressions, that molecular fragmentation is not included when a SCH or DCH is present because the time scale is, in this case, determined by the decay time of the vacancies which is much shorter than the fragmentation time.

The other dicationic configurations of  $N_2^{2+}$  are  $\{213, 213\}$ ,  $\{222, 222\}$ ,  $\{123, 213\}$ ,  $\{123, 222\}$ ,  $\{213, 222\}$ ,  $\{203, 223\}$ ,  $\{221, 223\}$ , and  $\{122, 223\}$ ; the involved molecular rate equations are formulated in analogy to the above scheme [54].

#### 2.4. Molecular nitrogen trication $N_2^{3+}$

Further photoionization or Auger decay of the molecular dication  $N_2^{2+}$  produces the trication  $N_2^{3+}$ . No bound states were found for  $N_2^{3+}$  ions in the midst of many Coulomb repulsive potentials [68]. Therefore, we assume that those  $N_2^{3+}$  ions with no core holes fragment into  $N^{2+}$  and  $N^+$  at the instant of their formation by Auger decay or photoionization. The probability for the formation of  $N_2^{3+}$  ions without core holes is small due to small valence ionization cross sections at the x-ray photon energy [69]. In contrast,  $N_2^{3+}$  with core holes is still treated as a molecule, i.e., no immediate fragmentation is assumed; the  $N_2^{3+}$  are only broken up by Auger decay or photoionization because of the faster time scale of Auger decay compared with molecular fragmentation.

For the triply charged molecular configurations, with a SCH and two valence holes, we have the exemplary rate equations

$$\frac{d\tilde{P}_{121,223}(t)}{dt} = \sigma_{121\leftarrow 221} \tilde{P}_{221,223}(t) J_X(t) + \sigma_{121\leftarrow 122} \tilde{P}_{122,223}(t) J_X(t)$$

$$\begin{aligned}
& - (\sigma_{121} + \sigma_{223}) \tilde{P}_{121,223}(t) J_X(t) + \Gamma_{121 \leftarrow 023} \tilde{P}_{023,223}(t) \\
& - \Gamma_{121} \tilde{P}_{121,223}(t) ,
\end{aligned} \tag{9}$$

$$\begin{aligned}
\frac{d\tilde{P}_{212,123}(t)}{dt} = & \sigma_{123 \leftarrow 223} \tilde{P}_{212,223}(t) J_X(t) + \sigma_{212 \leftarrow 213} \tilde{P}_{123,213}(t) J_X(t) \\
& + \sigma_{212 \leftarrow 222} \tilde{P}_{123,222}(t) J_X(t) - (\sigma_{212} + \sigma_{123}) \tilde{P}_{212,123}(t) J_X(t) \\
& + 2 \Gamma_{212 \leftarrow 123} \tilde{P}_{123,123}(t) - \Gamma_{123} \tilde{P}_{212,123}(t) ,
\end{aligned} \tag{10}$$

a tsDCH and a valence hole

$$\begin{aligned}
\frac{d\tilde{P}_{113,123}(t)}{dt} = & \sigma_{113 \leftarrow 213} \tilde{P}_{123,213}(t) J_X(t) + \sigma_{123 \leftarrow 223} \tilde{P}_{113,223}(t) J_X(t) \\
& + 2 \sigma_{113 \leftarrow 123} \tilde{P}_{123,123}(t) J_X(t) - (\sigma_{113} + \sigma_{123}) \\
& \times \tilde{P}_{113,123}(t) J_X(t) - (\Gamma_{113} + \Gamma_{123}) \tilde{P}_{113,123}(t) ,
\end{aligned} \tag{11}$$

a ssDCH and a valence hole

$$\begin{aligned}
\frac{d\tilde{P}_{013,223}(t)}{dt} = & \sigma_{013 \leftarrow 113} \tilde{P}_{113,223}(t) J_X(t) + \sigma_{013 \leftarrow 023} \tilde{P}_{023,223}(t) J_X(t) \\
& - (\sigma_{013} + \sigma_{223}) \tilde{P}_{013,223}(t) J_X(t) - \Gamma_{013} \tilde{P}_{013,223}(t) ,
\end{aligned} \tag{12}$$

and a ssDCH and a SCH

$$\begin{aligned}
\frac{d\tilde{P}_{023,123}(t)}{dt} = & 2 \sigma_{023 \leftarrow 123} \tilde{P}_{123,123}(t) J_X(t) + \sigma_{123 \leftarrow 223} \tilde{P}_{023,223}(t) J_X(t) \\
& - (\sigma_{023} + \sigma_{123}) \tilde{P}_{023,123}(t) J_X(t) - (\Gamma_{023} + \Gamma_{123}) \tilde{P}_{023,123}(t) .
\end{aligned} \tag{13}$$

The other tricationic configurations of  $\text{N}_2^{3+}$  are  $\{113, 213\}$ ,  $\{113, 222\}$ ,  $\{122, 213\}$ ,  $\{023, 213\}$ ,  $\{203, 123\}$ ,  $\{112, 223\}$ ,  $\{103, 223\}$ ,  $\{122, 222\}$ ,  $\{023, 222\}$ ,  $\{221, 123\}$ ,  $\{122, 123\}$ , and  $\{022, 223\}$ ; the resulting molecular rate equations are written accordingly [54].

### 2.5. Higher charge states of a nitrogen molecule

Molecular effects are centered around the steps described in section 2.1, 2.2, 2.3, and 2.4 [34]. For even higher charge states, the interaction is basically those of independent atoms and no molecular rate equations are formulated. Instead, immediate fragmentation is assumed for the molecular tetracation  $\text{N}_2^{4+}$  where the four charges are shared equally between the two nitrogen nuclei [64,65]. The probability of the fragments is funneled into the atomic rate equations which govern the time evolution from this point onwards [54].

## 3. Results and discussion

To predict the ion yields and the average charge state of  $\text{N}_2$  in intense and ultrafast x-rays, we use a number of computational parameters which were either taken from experiments [1,61] or calculated [34]. The x-ray field parameters used here are listed in table 1 and are the same as the ones in [1,34]. The expression for the beam profile



of LCLS pulses can be found in [34]. The dissociative photoionization cross sections of a SCH in  $N_2$  are known from experiments at third-generation synchrotrons [61]. From these we find [34] for the fragment ion ratios in (4) the values  $f_{N^{++}N^+} = 0.74$  and  $f_{N^+N^{2+}} = 1 - f_{N^{++}N^+} = 0.26$ ; we use them to parametrize our rate equations to ensure that the ion yields approach the values of SCH decay from synchrotrons in the limit of low x-ray intensities and fluences. Auger and fluorescence decay widths and the corresponding transition energies, electron binding energies, and one-x-ray-photon absorption cross sections for multiply-ionized N atoms can be found in [34] where they were determined with *ab initio* computations. The joint molecular and atomic rate equations form a system of ordinary first-order linear differential equations which is solved numerically with *Mathematica* [54, 55] with the initial condition that  $N_2$  is in its ground state, i.e.,  $\tilde{P}_{223,223}(-\infty) = 1$ , and all the other molecular states and all atomic states are unpopulated, i.e.,  $\tilde{P}_{ijk,\ell mn}(-\infty) = 0$  with  $0 \leq i, j, \ell, m \leq 2 \wedge 0 \leq k, n \leq 3 \wedge \neg(i = j = \ell = m = 2 \wedge k = n = 3)$  and  $P_{ijk}(-\infty) = 0$  with  $0 \leq i, j \leq 2 \wedge 0 \leq k \leq 3$ .

The ion yields of atomic fragments from molecules with a charge of  $1 \leq j \leq 7$  are the molecular ion yields

$$\tilde{Y}_j = \frac{P_j}{1 - P_0}, \quad (14)$$

which are experimentally measurable quantities and are defined as the renormalized charge-state probability where

$$P_j = \sum_{\substack{\ell+m+n=7-j \\ 0 \leq \ell, m \leq 2 \wedge 0 \leq n \leq 3}} P_{\ell mn}(\infty), \quad (15)$$

is the probability to find an atomic fragment with charge  $0 \leq j \leq 7$  for  $t \rightarrow \infty$  when molecular breakup is always assumed. From the ion yields (14), we calculate the average charge state via

$$\bar{q} = \sum_{j=1}^7 j \tilde{Y}_j; \quad (16)$$

it is an indicator of the amount of charge found on molecular fragments.

In the experiment, the beam line transmission is not particularly well determined due to beam transport losses, which leads to a large uncertainty in the pulse energy actually reaching the sample; we estimated that only 15%–35% of the nominal pulse energy arrived at the sample [1, 27, 34]. Therefore, the effective pulse energy  $E_P$  and the rate of molecular fragmentation  $\gamma$  [Equation (3) and (5)] in our calculations are unknown and need to be found by comparing theoretical results with experimental data. For this purpose, we jointly determine  $E_P$  and  $\gamma$  by minimizing the criterion

$$C_j(E_P, \gamma) = |\bar{q}_{\text{expt}} - \bar{q}_{\text{theo}}(E_P, \gamma)| + 16 |\tilde{Y}_{\text{expt},j} - \tilde{Y}_{\text{theo},j}(E_P, \gamma)|; \quad (17)$$

it comprises the absolute value of the difference between the experimental  $\bar{q}_{\text{expt}}$  and the theoretical  $\bar{q}_{\text{theo}}(E_P, \gamma)$  average charge state and the absolute value of 16 times the difference between the experimental  $\tilde{Y}_{\text{expt},j}$  and the theoretical  $\tilde{Y}_{\text{theo},j}(E_P, \gamma)$  ion yield of

**Table 1.** Parameters of the molecular rate-equation model. The LCLS nominal FWHM pulse duration is  $\tau_X$  and the effective pulse duration is  $\tau'_X$  [34]. A nominal pulse energy of 0.15 mJ is specified for 4 fs pulses and 0.26 mJ for the remaining three pulse durations of 7 fs, 80 fs, and 280 fs. The effective LCLS pulse energy from molecular rate equations is  $E_P$ , i.e., the energy which arrives at the sample. The fragmentation time for nominal pulse durations from an optimization (17) with respect to the  $N^+$  yield is  $\gamma_{N^+}^{-1}$  and with respect to the  $N^{2+}$  yield it is  $\gamma_{N^{2+}}^{-1}$ ; correspondingly  $\gamma'_{N^+}{}^{-1}$  and  $\gamma'_{N^{2+}}{}^{-1}$  are the fragmentation times for effective pulse durations. No fragmentation times could be determined for 4 fs and 7 fs pulses. The LCLS photon energy is 1100 eV.

$\tau_X$ [fs]	$\tau'_X$ [fs]	$E_P$ [mJ]	$\gamma_{N^+}^{-1}$ [fs]	$\gamma'_{N^+}{}^{-1}$ [fs]	$\gamma_{N^{2+}}^{-1}$ [fs]	$\gamma'_{N^{2+}}{}^{-1}$ [fs]
280	112	$0.38 \times 0.26$	246	95	201	76
80	40	$0.30 \times 0.26$	83	40	60	26
7	2.8	$0.16 \times 0.26$				
4	1.6	$0.23 \times 0.15$				

either  $N^+$  for  $j = 1$  or  $N^{2+}$  for  $j = 2$ . The second summand in (17) causes the criterion to have a fairly sharp global minimum where the prefactor of 16 is somewhat arbitrary but chosen large enough to ensure that the second summand makes a large contribution thus effecting a good agreement between experimental and theoretical average charge states provided that simultaneously also the chosen experimental and theoretical ion yield agree well; only  $N^+$  or  $N^{2+}$  ion yields (4) are considered in the second summand because only these are influence directly by  $\gamma$  [Equation (3) and (5)]. The ion yields from higher charge states are only indirectly impacted by fragmentation [34].

We list in table 1 the effective pulse energies and fragmentation times obtained by minimizing the criterion (17) for 80 fs and 280 fs nominal LCLS pulse durations. It was found that the nominal pulse durations specified by the accelerator electron beam parameters [1, 4] are substantially longer than the effective pulse durations at the sample [4, 70] for which values for the fragmentation time are also given. As the dependence of 4 fs and 7 fs pulses on  $\gamma$  is very weak, it was not possible to extract it from (17). In order to obtain the effective pulse energy for the short pulse durations,  $\gamma_{N^+}$  is used with the value from the nominal duration of the 280 fs pulses. The percentages of the nominal pulse energies that effectively arrive at the sample lie almost in the range of 15%–35% which was specified in the experiment [1]. The percentages in table 1 of this work have a close agreement with those of the fragmentation-matrix model in Table I of [34] which are 26%, 16%, 25%, and 31% for pulse durations of 4 fs, 7 fs, 80 fs and 280 fs, respectively. This means that the effective energy of the LCLS pulses arriving at the sample decreases with the shortening of the pulse. A reanalysis of the experimental data of [1] in [27] confirmed the predicted drop in the effective pulse energy.

Comparing  $\gamma_{N^+}^{-1}$  and  $\gamma_{N^{2+}}^{-1}$  for a specific pulse duration in table 1 reveals a noticeable difference which is due to the fact that different pathways contribute to these ion yields. For example,  $N^+$  ions are not only produced by (4a) but, e.g., also by valence

ionization of N; and  $N^{2+}$  ions do not only result from (4b) but, e.g., also from Auger decay of a SCH in a  $N^+$  ion. As neither  $N^+$  nor  $N^{2+}$  are solely produced by molecular fragmentation, this causes a systematic error, if we use (17), which can be estimated from the differences between the respective fragmentation times in table 1 for the same pulse duration. Another source of error are the variations of the fragmentation times for a specific ion yield with the pulse duration, e.g.,  $\gamma_{N^+}^{-1}$ , obtained from 80 fs and 280 fs pulses. This happens because the contribution of the pathways varies when the pulse duration is shortened as the peak x-ray intensity increases. The same holds true for the fragmentation times found from the effective pulse durations which are not known particularly precisely. In contrast to the theoretical results from the fragmentation-matrix model [34], which were found to depend on the pulse duration only weakly, for molecular rate equations the determination of the fragmentation rate  $\gamma$  is sensitive to the actual pulse duration. Overall, we find  $\gamma^{-1}$  to be in the range of 40–250 fs which is comparable to the value of  $\sim 100$  fs found in [63]. The fragmentation time  $\gamma^{-1}$  is much longer than the lifetime of a SCH of 6.73 fs [34] but is faster than the time for SCH production by photoionization for the 280 fs pulse which is 348 fs at the peak intensity. For the 4 fs short pulse, the lifetime of a SCH is comparable with the time between two photoionizations of 10.1 fs whereas the time of molecular fragmentation  $\gamma^{-1}$  is about an order of magnitude longer [54].

The ion yields of  $N_2$  from our molecular rate-equation model and the experiment are depicted in figure 2 where also theoretical ion yields are shown when certain DCH channels are closed. The results from the molecular rate equations agree nicely with the experimental data when all channels are included. Considering the results for which the DCH-containing channels are omitted, i.e., only the SCH channel is included, we see that the dominant features of the ion yields are reproduced. Specifically, the influence of DCHs is small for 280 fs pulses but DCHs have a substantial influence on the ion yields for the 4 fs pulse. This result is consistent with the analysis in Section V of [34]. The longer the pulse duration, the lower is the peak x-ray intensity of the pulse. Hence the rate of photoionization is fairly small for long pulses and Auger decay and molecular fragmentation are the dominant processes compared with DCH formation. On the contrary, for short pulses, the molecules are ionized faster resulting in DCHs but nuclear dynamics can be neglected because of the short pulse duration and valence charges are mostly shared equally between the two nitrogen atoms [34]. The artificial closing of DCH channels inhibits x-ray absorption and thus leads to an underestimation of the amount of ionization which means that the ion yields of low charge states in figure 2 are higher than the ones from the complete model and the higher charge states are lower, respectively.

Merits of the molecular rate-equation model over the fragmentation matrix model from [34] are that the former takes explicitly the time scale of molecular fragmentation into account and offers a description of the dynamics of the population of charge states whereas the latter provides only fragmentation constants. In order to reveal the important role of the fragmentation rate introduced in the molecular rate-equation

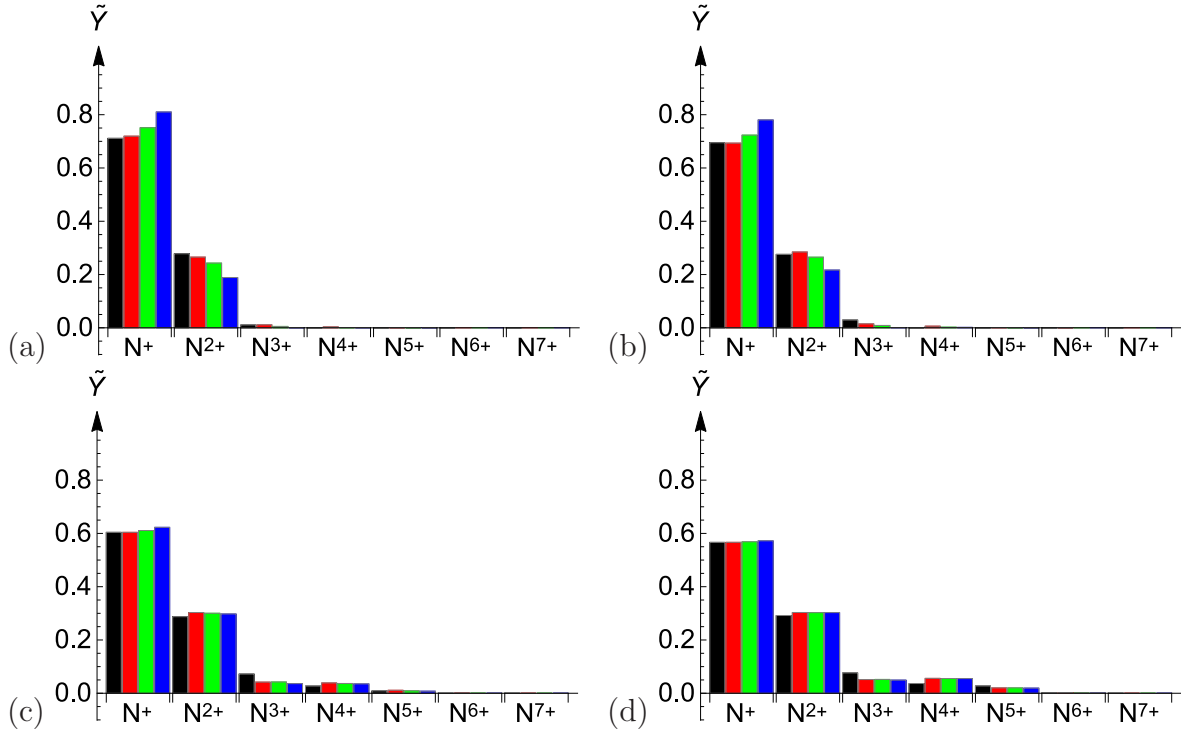


**Figure 2.** (Color) Ion yields of  $N_2$  ionized by LCLS x-rays with FWHM durations of (a) 4 fs, (b) 7 fs, (c) 80 fs, and (d) 280 fs. Experimental data (**black** bars); results of the molecular rate-equation model with all channels included (**red** bars), only with SCH and tsDCH channels included (**green** bars), and only with SCH channels included (**blue** bars). The fragmentation time of the molecular dication  $N_2^{2+}$  is  $\gamma^{-1} = 246$  fs for all pulses but 80 fs pulses for which  $\gamma^{-1} = 83$  fs is used. Other parameters are taken from table 1.

model [Equation (3) and (5)], in figure 3, a comparison of the ion yields is shown which are obtained from our molecular rate-equation model in the two extreme cases of  $\gamma \rightarrow \infty$  and  $\gamma = 0$  together with the results of the single-atom model and the experimental data. When immediate fragmentation at the instant of the formation of the metastable molecular dication  $N_2^{2+}$  is assumed i.e.,  $\gamma \rightarrow \infty$ , the molecular rate-equation model still gives similar ion yields as the experimental data. Specifically, the theoretical ion yields follow the same trend as the experimental ones. Yet we see clearly from figure 3, that the rather good agreement for 4 fs pulses becomes progressively worse for longer pulses. This observation reveals the increasing influence of the fragmentation time scale which eventually becomes comparable with the FWHM duration of the long pulses. As molecular breakup occurs immediately in (3) and (5) and the hierarchy of molecular rate equations is quenched at (3) because all probability is funneled into the atomic rate equation (5), several of the molecular rate equations for the trication are thus not used. Conversely, the other limit of the fragmentation time scale is  $\gamma = 0$  which means that fragmentation of the metastable molecular dication  $N_2^{2+}$  is neglected. One can see clearly from figure 3 the large differences between the experimental results and the theoretical

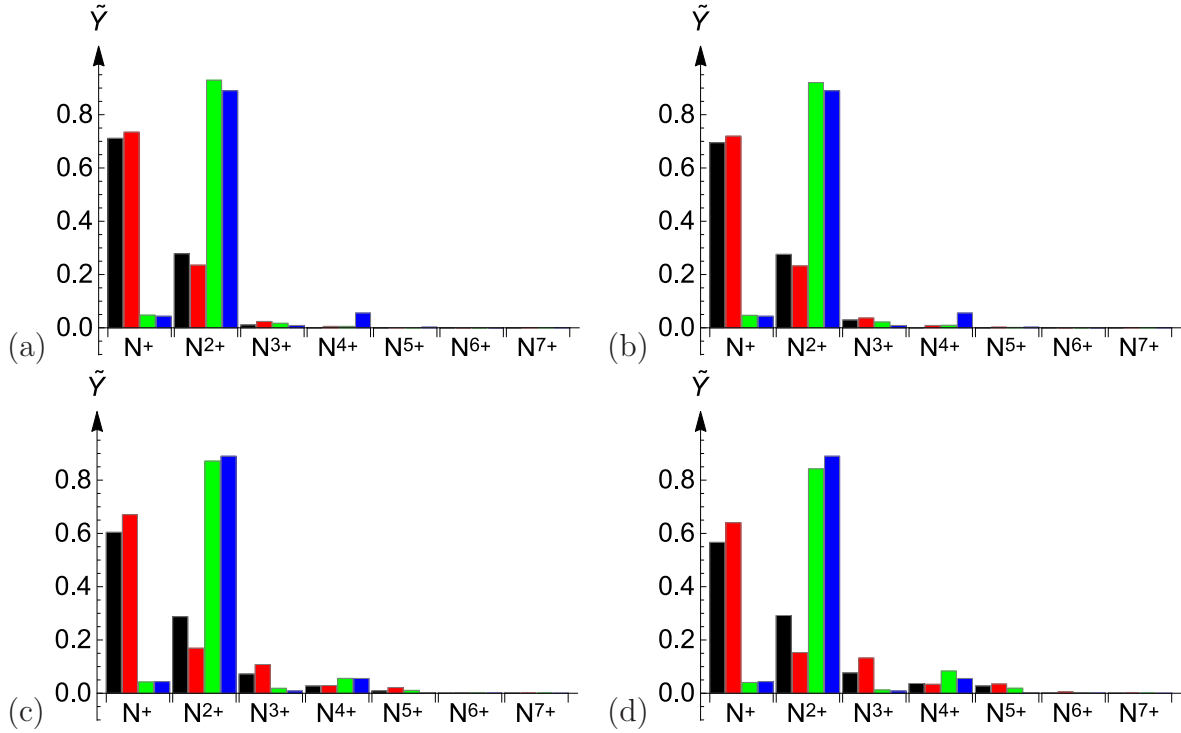


**Figure 3.** (Color) Ion yields of  $N_2$  ionized by LCLS x-rays with FWHM durations of (a) 4 fs, (b) 7 fs, (c) 80 fs, and (d) 280 fs. We display experimental data (**black** bars) alongside theoretical results of the molecular rate-equation model with all channels for  $\gamma \rightarrow \infty$  (**red** bars) and for  $\gamma = 0$  (**green** bars). Further, we give theoretical results of the atomic rate-equation model (**blue** bars). Other parameters are taken from table 1.

calculations. The ion yields in this limit agree well with the atomic rate-equation model but poorly with the experimental data. Specifically, the molecular rate equations in this limit do not describe the experimental observation that the ion yields of the lowly charged ions are higher than those of the highly charged ions (see [34] for details of the single-atom model). We also observe in figure 3 that the variation of the ion yields with the pulse duration is substantially reduced for the atomic rate equations which indicates that the heightened sensitivity to the pulse duration is due to molecular fragmentation. In other words, the metastability of the molecular dication  $N_2^{2+}$  plays an essential role in the interaction of  $N_2$  with x-ray pulses and its finite rate of dissociation must not be neglected.

In figure 4, we display the average charge state  $\bar{q}$  of (16) obtained from the experiment [1] and the molecular rate-equation model. Figure 4 shows that the model reproduces very well the decreasing tendency of  $\bar{q}$  with the decrease of the pulse duration. This comes to us as no surprise because we fitted (17) the theoretical  $\bar{q}$  to the experimental value in order to determine the effective pulse energy at the sample. Yet the results for which certain DCH channels are closed provide novel insights. Inspecting figure 4, we find that the SCH channel determines the main character of

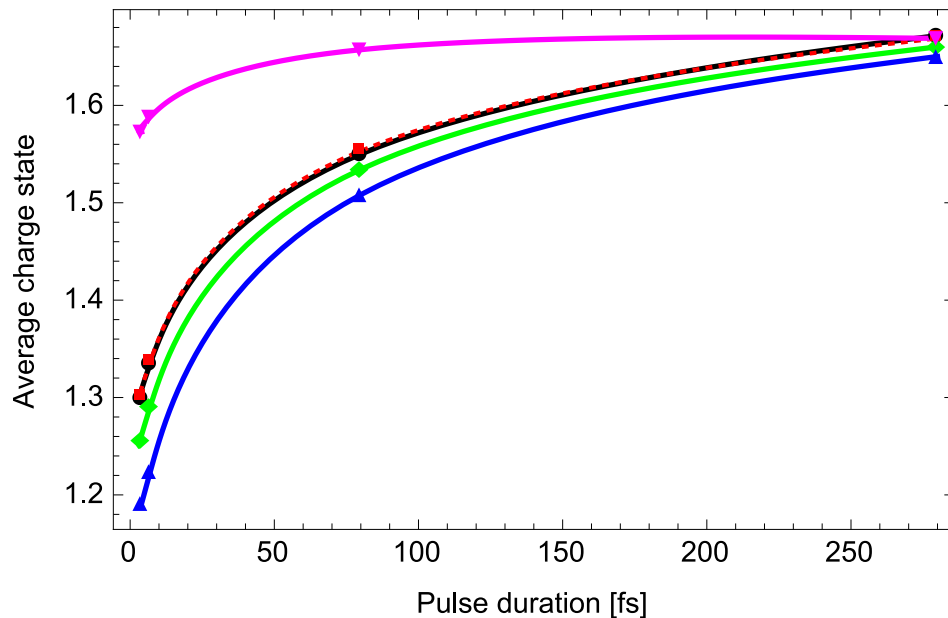


**Figure 4.** (Color) Average charge state  $\bar{q}$  [Equation (16)] of  $N_2$  ionized with LCLS pulses of varying duration. The measured and computed data points are shown and connected by spline interpolation. The experimental  $\bar{q}$  is shown as **black** circles, the theoretical  $\bar{q}$ , calculated with molecular rate equations is shown as **red** squares (SCH, tsDCH, and ssDCH channels), **green** diamonds (only SCH and tsDCH channels), **blue** triangles up (only SCH channels), and **magenta** triangles down (constant pulse energy, SCH, tsDCH, and ssDCH channels). The parameters are the same as in figure 2.

the dependence of  $\bar{q}$  on the pulse duration. It describes well the nuclear and electronic dynamics of  $N_2$  for long pulses. That is because for, e.g., the 280 fs pulse, Auger decay is the fastest process; a core hole formed by photoionization of an inner-shell electron is typically refilled by Auger decay before another core electron is photoionized. However, the restriction to only SCH channels significantly underestimates  $\bar{q}$  for short pulses compared with the experimental result which can only be obtained by including the molecular configurations with tsDCH and ssDCH. This means that there is an appreciable probability of ionization of a second core electron before Auger decay of the core hole occurs. Furthermore, one can see from figure 2 and figure 4 that tsDCHs make a stronger contribution than ssDCHs because of the larger cross section for the formation of a tsDCH—as the x-ray photoabsorption cross section of an atom with no core hole is larger than that with a single core hole—and the lifetime of tsDCH is longer compared with the lifetime of a ssDCH [34].

Overall, there is a drop in  $\bar{q}$  for short pulses compared with long pulses in figure 4. This *observed* frustrated absorption is ascribed to three effects: first, the decrease in the x-ray absorption cross section due to SCH and DCH formation, i.e., the effect of frustrated absorption [1]¶, second, due to a predominantly symmetric sharing of the

¶ This is in contrast to [34] where we focused on the sharing of charges due to molecular breakup on

charges for short pulses upon breakup as the molecular ion remains intact during the interaction in contrast to long pulses with fragmentation in the course of the interaction, and, third, the variation in the pulse energy at the sample which drops noticeably with shortening pulse duration [Table 1]. We also show  $\bar{q}$  in figure 4 when the pulse energy is constant. In this case, the drop of  $\bar{q}$  is only caused by the change of the breakup pattern and the effect of frustrated absorption. Considering only 4 fs and 7 fs pulses, there ought to be no significant change of the breakup pattern as the time scale for molecular dissociation of the metastable  $\text{N}_2^{2+}$  is much longer than the pulse durations. Nonetheless, there is a pronounced drop of  $\bar{q}$  for 4 fs pulse compared with 7 fs pulses which we ascribe entirely to frustrated absorption.

Figure 4 of this work corresponds to figure 4 of [34] which shows the experimental  $\bar{q}$  together with  $\bar{q}$  from the single-atom model that represents an upper limit to  $\bar{q}$ , the symmetric-sharing model which provides a lower limit to  $\bar{q}$ , and the fragmentation-matrix model that reproduces the experimental  $\bar{q}$  very well for short pulses but is less accurate for longer pulses as the fragmentation time scale is not explicitly included in the model. The agreement between the curves from the fragmentation-matrix model and the molecular rate-equation model is not a coincidence; it shows that the main physical effects are described.

Good agreement between theoretical calculation and experimental measurement of the ion yields and the average charge state of  $\text{N}_2$  for LCLS pulses with varying durations was also obtained in [1] saying that molecular rate equations were used. However, there, the molecular valence charge dynamics is modeled differently to here because there  $\text{N}_2^{4+}$  ions were assumed to fragment into  $\text{N}^{3+} + \text{N}^+$  or  $\text{N}^{2+} + \text{N}^{2+}$  with different ratios of  $\text{N}^{3+} + \text{N}^+$  versus  $\text{N}^{2+} + \text{N}^{2+}$ —depending on whether DCH decay or two photoionization with Auger decay cycles occurred—which were claimed to be adjusted to obtain the best agreement with the experimental data in the calculation there. Furthermore, there the effective pulse energy at the sample was adjusted in the range 17%–21% of the nominal pulse energy—which was *always* [table 1] taken to be 0.26 mJ in [1]—for pulses with FWHM durations of 4 fs, 7 fs, 80 fs, and 280 fs. Our computations reveal a stronger dependence of the average charge state on the pulse energy in the range 16%–38% of the nominal value for the pulse energy of different durations where the nominal pulse energy for 4 fs pulses was 0.15 mJ and 0.26 mJ otherwise [table 1]. The differences between the model discussed here and the model of [1] cannot be explained by the fact that SASE-type pulses were used in [1] instead of pulses with a Gaussian temporal shape employed here. Namely, the analysis in [34] reveals that the impact of the spikiness of SASE pulses compared with a Gaussian pulse is small and may be neglected in good approximation. We believe that three aspects of our model cause the observed differences: first, all possible one-photon absorption and decay channels of an N atom are determined from *ab initio* computations [34] and are included in our model, second, the molecular configurations up to  $\text{N}_2^{4+}$  are treated, and, third, the crucial dynamics

of dissociation of the metastable molecular dication  $\text{N}_2^{2+}$  is considered by introducing phenomenologically the fragmentation rate  $\gamma$ .

#### 4. Conclusion

We describe the interaction of intense and ultrafast x-rays with  $\text{N}_2$ . For this purpose, we lay the theoretical foundation for the description of multi-x-ray-photon absorption by molecules in rate-equation approximation and investigate theoretically the quantum dynamics of  $\text{N}_2$  exposed to x-ray pulses from LCLS. The results are determined by the competition between photoabsorption, decay processes, and molecular dissociation for x-ray pulses of varying duration and similar nominal pulse energy. Molecular configurations up to trications are included in the model taking into account the fragmentation dynamics of the metastable molecular dications and the redistribution of the valence electrons between the two atomic nuclei upon breakup. Atomic fragments after dissociation of the molecule are treated by atomic rate equations, i.e., no molecular effects are regarded anymore. The molecular rate-equation model describes the ionization dynamics observed and allows us to calculate theoretical ion yields and the average charge state which are then compared with the corresponding experimental quantities. Thereby, the effective pulse energy at the sample and the rate of fragmentation of the molecular dication  $\text{N}_2^{2+}$  are determined from a comparison of theoretical with experimental data. We find a substantial progression in the effective pulse energy which decreases pronouncedly from long to short pulses. The ion yields and effective pulse energies at the sample from the molecular rate equations agree well with those obtained previously with the fragmentation-matrix model of [34].

In [1] frustrated absorption was *observed* as a drop of the average charge state for short pulses compared with long pulses. There the most pronounced impact on the average charge state is due to the variation of the effective pulse energy as our previous [34] and present analysis reveals. Furthermore, for short pulses the molecular ions remain intact and fragment mostly in terms of symmetric sharing of charges whereas for long pulses fragmentation occurs frequently prior further absorption of x-rays leading to higher charge states in the latter case compared with the former. The effect of frustrated absorption describes the situation that core-hole formation reduces the probability for further x-ray absorption. It makes a significant contribution for short pulses compared with long pulses as DCH channels are more important in the former. Specifically, we find for long pulses with moderate x-ray intensity that photoabsorption is the slowest process; it is slower than the dissociation of the metastable dications  $\text{N}_2^{2+}$ . Molecular configurations with SCHs dominate where Auger decay quickly refills SCHs and thus increase the chance for further photoabsorption in the course of the interaction with the pulse because the photoionization cross section of a filled core shell is larger than the one of an only partially filled core shell. Conversely, for short pulses with high x-ray intensities, the rates of Auger decay and photoionization are comparable. In this case, there is a much larger probability for the production of DCHs



by sequential absorption of two x-rays within the lifetime of the core hole. Therefore, further x-ray absorption is reduced—compared with longer pulses of the same effective pulse energy—causing a smaller population of higher charge states. Thus frustrated absorption results in a pronounced drop of the average charge state in addition to the variation of the effective pulse energy and the variation of fragmentation patterns.

We would like to point out that our molecular rate-equation model works well for x-ray pulses at a photon energy of 1100 eV. We anticipate that the model remains applicable for lower photon energies up to the point when the photon energy still exceeds the highest ionization potential in the model of 667.05 eV for the ionization of the last *K*-shell electron of an otherwise electron-bare nucleus [34] as then resonances still play no significant role. Yet more experimental data are needed in order to assess whether our model stays valid for photon energies higher than 1100 eV because then the single-electron response model may become insufficient and multielectron effects such as shake off processes are noticeable [4]. Similar models to the ones discussed in [34] and here should be used to investigate other diatomic molecules in order to find out how general our approach is and whether also heteronuclear molecules are well described. Also the role of interatomic electronic decay [71] ought to be investigated in the future. We are confident that our theory can even be extended to molecules with more than two atoms.

## Acknowledgments

We are grateful to Mau Hsiung Chen (陳茂雄), Ryan N. Coffee, Li Fang (方力), Matthias Hoener, and Christoph H. Keitel for helpful discussions. J-CL thanks for support by the National Science Foundation of China under grant Nos. 11204078 and 11574082, and the Fundamental Research Funds for the Central Universities of China under grant No. 2015MS54. CB was supported by the National Science Foundation under grant Nos. PHY-0701372 and PHY-0449235 and by a Marie Curie International Reintegration Grant within the 7<sup>th</sup> European Community Framework Program (call identifier: FP7-PEOPLE-2010-RG, proposal No. 266551). NB is grateful for funding by the Office of Basic Energy Sciences, Office of Science, U.S. Department of Energy, under Contract No. DE-SC0012376. Portions of this research were carried out at the Linac Coherent Light Source (LCLS) at SLAC National Accelerator Laboratory. LCLS is an Office of Science User Facility operated for the U.S. Department of Energy Office of Science by Stanford University. JPC and JMG were supported through both the LCLS and The PULSE Institute for Ultrafast Energy Science at the SLAC National Accelerator Laboratory by the U.S. Department of Energy, Office of Basic Energy Sciences.

## References

- [1] Matthias Hoener, Li Fang, Oleg Kornilov, Oliver Gessner, Stephen T. Pratt, Markus Gühr, Elliot P. Kanter, Cosmin Blaga, Christoph Bostedt, John D. Bozek, Philip H. Bucksbaum, Christian Buth, Mau Chen, Ryan Coffee, James Cryan, Louis DiMauro, Michael Glownia, Erik Hosler,

- Edwin Kukk, Stephen R. Leone, Brian McFarland, Marc Messerschmidt, Brendan Murphy, Vladimir Petrovic, Daniel Rolles, and Nora Berrah. Ultraintense x-ray induced ionization, dissociation, and frustrated absorption in molecular nitrogen. *Phys. Rev. Lett.*, 104:253002, 2010.
- [2] Li Fang, Matthias Hoener, Oliver Gessner, Francesco Tarantelli, Stephen T. Pratt, Oleg Kornilov, Christian Buth, Markus Gühr, Elliot P. Kanter, Christoph Bostedt, John D. Bozek, Philip H. Bucksbaum, Mau Chen, Ryan Coffee, James Cryan, Michael Glowina, Edwin Kukk, Stephen R. Leone, and Nora Berrah. Double core hole production in  $N_2$ : Beating the Auger clock. *Phys. Rev. Lett.*, 105:083005, 2010.
- [3] James P. Cryan, James M. Glowina, Jakob Andreasson, Ali Belkacem, Nora Berrah, Cosmin I. Blaga, Christoph Bostedt, John Bozek, Christian Buth, Louis F. DiMauro, Li Fang, Oliver Gessner, Markus Guehr, Janos Hajdu, Markus P. Hertlein, Matthias Hoener, Oleg Kornilov, Jonathan P. Marangos, Anne M. March, Brian K. McFarland, Hamed Merdji, Vladimir S. Petrović, Chandra Raman, Dipanwita Ray, David Reis, Francesco Tarantelli, Mariano Trigo, James L. White, William White, Linda Young, Philip H. Bucksbaum, and Ryan N. Coffee. Auger electron angular distribution of double core hole states in the molecular reference frame. *Phys. Rev. Lett.*, 105:083004, 2010.
- [4] L. Young, E. P. Kanter, B. Krässig, Y. Li, A. M. March, S. T. Pratt, R. Santra, S. H. Southworth, N. Rohringer, L. F. DiMauro, G. Doumy, C. A. Roedig, N. Berrah, L. Fang, M. Hoener, P. H. Bucksbaum, J. P. Cryan, S. Ghimire, J. M. Glowina, D. A. Reis, J. D. Bozek, C. Bostedt, and M. Messerschmidt. Femtosecond electronic response of atoms to ultra-intense x-rays. *Nature*, 466:56–61, 2010.
- [5] I. A. Vartanyants, A. Singer, A. P. Mancuso, O. M. Yefanov, A. Sakdinawat, Y. Liu, E. Bang, G. J. Williams, G. Cadenazzi, B. Abbey, H. Sinn, D. Attwood, K. A. Nugent, E. Weckert, T. Wang, D. Zhu, B. Wu, C. Graves, A. Scherz, J. J. Turner, W. F. Schlotter, M. Messerschmidt, J. Lüning, Y. Acremann, P. Heimann, D. C. Mancini, V. Joshi, J. Krzywinski, R. Soufli, M. Fernandez-Perea, S. Hau-Riege, A. G. Peele, Y. Feng, O. Krupin, S. Moeller, and W. Wurth. Coherence properties of individual femtosecond pulses of an x-ray free-electron laser. *Phys. Rev. Lett.*, 107:144801, 2011.
- [6] S. Bernitt, G. V. Brown, J. K. Rudolph, R. Steinbrügge, A. Graf, M. Leutenegger, S. W. Epp, S. Eberle, K. Kubiček, V. Mäckel, M. C. Simon, E. Träbert, E. W. Magee, C. Beilmann, N. Hell, S. Schippers, A. Müller, S. M. Kahn, A. Surzhykov, Z. Harman, C. H. Keitel, J. Clementson, F. S. Porter, W. Schlotter, J. J. Turner, J. Ullrich, P. Beiersdorfer, and J. R. Crespo López-Urrutia. An unexpectedly low oscillator strength as the origin of the Fe XVII emission problem. *Nature*, 492:225–228, 2012.
- [7] T. E. Glover, D. M. Fritz, M. Cammarata, T. K. Allison, Sinisa Coh, J. M. Feldkamp, H. Lemke, D. Zhu, Y. Feng, R. N. Coffee, M. Fuchs, S. Ghimire, J. Chen, S. Shwartz, D. A. Reis, S. E. Harris, and J. B. Hastings. X-ray and optical wave mixing. *Nature*, 488:603–608, 2012.
- [8] Sébastien Boutet, Lukas Lomb, Garth J. Williams, Thomas R. M. Barends, Andrew Aquila, R. Bruce Doak, Uwe Weierstall, Daniel P. DePonte, Jan Steinbrener, Robert L. Shoeman, Marc Messerschmidt, Anton Barty, Thomas A. White, Stephan Kassemeyer, Richard A. Kirian, M. Marvin Seibert, Paul A. Montanez, Chris Kenney, Ryan Herbst, Philip Hart, Jack Pines, Gunther Haller, Sol M. Gruner, Hugh T. Philipp, Mark W. Tate, Marianne Hromalik, Lucas J. Koerner, Niels van Bakel, John Morse, Wilfred Ghonsalves, David Arnlund, Michael J. Bogan, Carl Caleman, Raimund Fromme, Christina Y. Hampton, Mark S. Hunter, Linda C. Johansson, Gergely Katona, Christopher Kupitz, Mengning Liang, Andrew V. Martin, Karol Nass, Lars Redecke, Francesco Stellato, Nicusor Timneanu, Dingjie Wang, Nadia A. Zatsepin, Donald Schafer, James Defever, Richard Neutze, Petra Fromme, John C. H. Spence, Henry N. Chapman, and Ilme Schlichting. High-resolution protein structure determination by serial femtosecond crystallography. *Science*, 337:362–364, 2012.
- [9] Nina Rohringer, Duncan Ryan, Richard A. London, Michael Purvis, Felicie Albert, James Dunn,

- John D. Bozek, Christoph Bostedt, Alexander Graf, Randal Hill, Stefan P. Hau-Riege, and Jorge J. Rocca. Atomic inner-shell x-ray laser at 1.46 nm pumped by an x-ray free electron laser. *Nature*, 481:488–491, 2012.
- [10] P. Salén, P. van der Meulen, H. T. Schmidt, R. D. Thomas, M. Larsson, R. Feifel, M. N. Piancastelli, L. Fang, B. Murphy, T. Osipov, N. Berrah, E. Kukk, K. Ueda, J. D. Bozek, C. Bostedt, S. Wada, R. Richter, V. Feyer, and K. C. Prince. Experimental verification of the chemical sensitivity of two-site double core-hole states formed by an x-ray free-electron laser. *Phys. Rev. Lett.*, 108:153003, 2012.
- [11] H. Thomas, A. Helal, K. Hoffmann, N. Kandadai, J. Keto, J. Andreasson, B. Iwan, M. Seibert, N. Timneanu, J. Hajdu, M. Adolph, T. Gorkhover, D. Rupp, S. Schorb, T. Möller, G. Doumy, L. F. DiMauro, M. Hoener, B. Murphy, N. Berrah, M. Messerschmidt, J. Bozek, C. Bostedt, and T. Ditmire. Explosions of xenon clusters in ultraintense femtosecond x-ray pulses from the LCLS free electron laser. *Phys. Rev. Lett.*, 108:133401, 2012.
- [12] D. Starodub, A. Aquila, S. Bajt, M. Barthelmess, A. Barty, C. Bostedt, J. D. Bozek, N. Coppola, R. B. Doak, S. W. Epp, B. Erk, L. Foucar, L. Gumprecht, C. Y. Hampton, A. Hartmann, R. Hartmann, P. Holl, S. Kassemeyer, N. Kimmel, H. Laksmono, M. Liang, N. D. Loh, L. Lomb, A. V. Martin, K. Nass, C. Reich, D. Rolles, B. Rudek, A. Rudenko, J. Schulz, R. L. Shoeman, R. G. Sierra, H. Soltau, J. Steinbrener, F. Stellato, S. Stern, G. Weidenspointner, M. Frank, J. Ullrich, L. Strüder, I. Schlichting, H. N. Chapman, J. C. H. Spence, and M. J. Bogan. Single-particle structure determination by correlations of snapshot x-ray diffraction patterns. *Nat. Commun.*, 3:1276, 2012.
- [13] B. F. Murphy, L. Fang, M.-H. Chen, J. D. Bozek, E. Kukk, E. P. Kanter, M. Messerschmidt, T. Osipov, and N. Berrah. Multiphoton  $L$ -shell ionization of  $H_2S$  using intense x-ray pulses from a free-electron laser. *Phys. Rev. A*, 86:053423, 2012.
- [14] Vladimir S. Petrović, Marco Siano, James L. White, Nora Berrah, Christoph Bostedt, John D. Bozek, Douglas Broege, Max Chalfin, Ryan N. Coffee, James Cryan, Li Fang, Joseph P. Farrell, Leszek J. Frasinski, James M. Glowina, Markus Gühr, Matthias Hoener, David M. P. Holland, Jaehee Kim, Jonathan P. Marangos, Todd Martinez, Brian K. McFarland, Russell S. Minns, Shungo Miyabe, Sebastian Schorb, Roseanne J. Sension, Limor S. Spector, Richard Squibb, Hongli Tao, Jonathan G. Underwood, and Philip H. Bucksbaum. Transient x-ray fragmentation: probing a prototypical photoinduced ring opening. *Phys. Rev. Lett.*, 108:253006, 2012.
- [15] T. Gorkhover, M. Adolph, D. Rupp, S. Schorb, S. W. Epp, B. Erk, L. Foucar, R. Hartmann, N. Kimmel, K.-U. Kühnel, D. Rolles, B. Rudek, A. Rudenko, R. Andritschke, A. Aquila, J. D. Bozek, N. Coppola, T. Erke, F. Filsinger, H. Gorke, H. Graafsma, L. Gumprecht, G. Hauser, S. Herrmann, H. Hirsemann, A. Hömke, P. Holl, C. Kaiser, F. Krasniqi, J.-H. Meyer, M. Matysek, M. Messerschmidt, D. Miessner, B. Nilsson, D. Pietschner, G. Potdevin, C. Reich, G. Schaller, C. Schmidt, F. Schopper, C. D. Schröter, J. Schulz, H. Soltau, G. Weidenspointner, I. Schlichting, L. Strüder, J. Ullrich, T. Möller, and C. Bostedt. Nanoplasma dynamics of single large xenon clusters irradiated with superintense x-ray pulses from the Linac Coherent Light Source free-electron laser. *Phys. Rev. Lett.*, 108:245005, 2012.
- [16] Sebastian Schorb, Daniela Rupp, Michelle L. Swiggers, Ryan N. Coffee, Marc Messerschmidt, Garth Williams, John D. Bozek, Shin-Ichi Wada, Oleg Kornilov, Thomas Möller, and Christoph Bostedt. Size-dependent ultrafast ionization dynamics of nanoscale samples in intense femtosecond x-ray free-electron-laser pulses. *Phys. Rev. Lett.*, 108:233401, 2012.
- [17] Lars Redecke, Karol Nass, Daniel P. DePonte, Thomas A. White, Dirk Rehders, Anton Barty, Francesco Stellato, Mengning Liang, Thomas R.M. Barends, Sébastien Boutet, Garth J. Williams, Marc Messerschmidt, M. Marvin Seibert, Andrew Aquila, David Arnlund, Sasa Bajt, Torsten Barth, Michael J. Bogan, Carl Caleman, Tzu-Chiao Chao, R. Bruce Doak, Holger Fleckenstein, Matthias Frank, Raimund Fromme, Lorenzo Galli, Ingo Grotjohann, Mark S. Hunter, Linda C. Johansson, Stephan Kassemeyer, Gergely Katona, Richard A. Kirian, Rudolf Koopmann, Chris Kupitz, Lukas Lomb, Andrew V. Martin, Stefan Mogk, Richard Neutze,

- Robert L. Shoeman, Jan Steinbrener, Nicusor Timneanu, Dingjie Wang, Uwe Weierstall, Nadia A. Zatsepin, John C. H. Spence, Petra Fromme, Ilme Schlichting, Michael Duszynko, Christian Betzel, and Henry N. Chapman. Natively inhibited trypanosoma brucei cathepsin B structure determined by using an x-ray laser. *Science*, 339:227–230, 2013.
- [18] S. Schulz, I. Grguraš, C. Behrens, H. Bromberger, J. T. Costello, M. K. Czwalińska, M. Felber, M. C. Hoffmann, M. Ilchen, H. Y. Liu, T. Mazza, M. Meyer, S. Pfeiffer, P. Prędki, S. Schefer, C. Schmidt, U. Wegner, H. Schlarb, and A. L. Cavalieri. Femtosecond all-optical synchronization of an X-ray free-electron laser. *Nat. Commun.*, 6:5938, 2015.
- [19] J. Arthur, P. Anfinrud, P. Audebert, K. Bane, I. Ben-Zvi, V. Bharadwaj, R. Bionta, P. Bolton, M. Borland, P. H. Bucksbaum, R. C. Cauble, J. Clendenin, M. Cornacchia, G. Decker, P. Den Hartog, S. Dierker, D. Dowell, D. Dungan, P. Emma, I. Evans, G. Faigel, R. Falcone, W. M. Fawley, M. Ferrario, A. S. Fisher, R. R. Freeman, J. Frisch, J. Galayda, J.-C. Gauthier, S. Gierman, E. Gluskin, W. Graves, J. Hajdu, J. Hastings, K. Hodgson, Z. Huang, R. Humphry, P. Ilinski, D. Imre, C. Jacobsen, C.-C. Kao, K. R. Kase, K.-J. Kim, R. Kirby, J. Kirz, L. Klaisner, P. Krejčík, K. Kulander, O. L. Landen, R. W. Lee, C. Lewis, C. Limborg, E. I. Lindau, A. Lumpkin, G. Materlik, S. Mao, J. Miao, S. Mochrie, E. Moog, S. Milton, G. Mulholland, K. Nelson, W. R. Nelson, R. Neutze, A. Ng, D. Nguyen, H.-D. Nuhn, D. T. Palmer, J. M. Paterson, C. Pellegrini, S. Reiche, M. Renner, D. Riley, C. V. Robinson, S. H. Rokni, S. J. Rose, J. Rosenzweig, R. Ruland, G. Ruocco, D. Saenz, S. Sasaki, D. Sayre, J. Schmerge, D. Schneider, C. Schroeder, L. Serafini, F. Sette, S. Sinha, D. van der Spoel, B. Stephenson, G. Stupakov, M. Sutton, A. Szöke, R. Tatchyn, A. Toor, E. Trakhtenberg, I. Vasserman, N. Vinokurov, X. J. Wang, D. Waltz, J. S. Wark, E. Weckert, Wilson-Squire Group, H. Winick, M. Woodley, A. Wootton, M. Wulff, M. Xie, R. Yotam, L. Young, and A. Zewail. Linac Coherent Light Source (LCLS): Conceptual Design Report. Technical Report SLAC-R-593, UC-414, Stanford Linear Accelerator Center (SLAC), Menlo Park, California, USA, April 2002.
- [20] P. Emma, R. Akre, J. Arthur, R. Bionta, C. Bostedt, J. Bozek, A. Brachmann, P. Bucksbaum, R. Coffee, F.-J. Decker, Y. Ding, D. Dowell, S. Edstrom, J. Fisher, A. Frisch, S. Gilevich, J. Hastings, G. Hays, Ph. Hering, Z. Huang, R. Iverson, H. Loos, M. Messerschmidt, A. Miahnahri, S. Moeller, H.-D. Nuhn, G. Pile, D. Ratner, J. Rzepiela, D. Schultz, T. Smith, P. Stefan, H. Tompkins, J. Turner, J. Welch, W. White, J. Wu, G. Yocky, and J. Galayda. First lasing and operation of an ångström-wavelength free-electron laser. *Nature Photon.*, 4:641–647, 2010.
- [21] Bernhard W. Adams, Christian Buth, Stefano M. Cavaletto, Jörg Evers, Zoltán Harman, Christoph H. Keitel, Adriana Pálffy, Antonio Picón, Ralf Röhlsberger, Yuri Rostovtsev, and Kenji Tamasaku. X-ray quantum optics. *J. Mod. Opt.*, 60:2–21, 2013.
- [22] G. Doumy, C. Roedig, S.-K. Son, C. I. Blaga, A. D. DiChiara, R. Santra, N. Berrah, C. Bostedt, J. D. Bozek, P. H. Bucksbaum, J. P. Cryan, L. Fang, S. Ghimire, J. M. Glowacki, M. Hoener, E. P. Kanter, B. Krässig, M. Kuebel, M. Messerschmidt, G. G. Paulus, D. A. Reis, N. Rohringer, L. Young, P. Agostini, and L. F. DiMauro. Nonlinear atomic response to intense ultrashort x rays. *Phys. Rev. Lett.*, 106:083002, 2011.
- [23] Yasuo Nabekawa, Hirokazu Hasegawa, Eiji J. Takahashi, and Katsumi Midorikawa. Production of doubly charged helium ions by two-photon absorption of an intense sub-10-fs soft x-ray pulse at 42 eV photon energy. *Phys. Rev. Lett.*, 94:043001, 2005.
- [24] E. P. Kanter, B. Krässig, Y. Li, A. M. March, P. Ho, N. Rohringer, R. Santra, S. H. Southworth, L. F. DiMauro, G. Doumy, C. A. Roedig, N. Berrah, L. Fang, M. Hoener, P. H. Bucksbaum, S. Ghimire, D. A. Reis, J. D. Bozek, C. Bostedt, M. Messerschmidt, and L. Young. Unveiling and driving hidden resonances with high-fluence, high-intensity x-ray pulses. *Phys. Rev. Lett.*, 107:233001, 2011.
- [25] Stefano M. Cavaletto, Christian Buth, Zoltán Harman, Elliot P. Kanter, Stephen H. Southworth, Linda Young, and Christoph H. Keitel. Resonance fluorescence in ultrafast and intense x-ray free electron laser pulses. *Phys. Rev. A*, 86:033402, 2012.

- [26] F. Krasniqi, B. Najjari, L. Strüder, D. Rolles, A. Voitkiv, and J. Ullrich. Imaging molecules from within: ultrafast angström-scale structure determination of molecules via photoelectron holography using free-electron lasers. *Phys. Rev. A*, 81:033411, 2010.
- [27] Li Fang, Timur Osipov, Brendan Murphy, Francesco Tarantelli, Edwin Kukk, James Cryan, Philip H. Bucksbaum, Ryan N. Coffee, Mau Chen, Christian Buth, and Nora Berrah. Multiphoton ionization as a clock to reveal molecular dynamics with intense short x-ray free electron laser pulses. *Phys. Rev. Lett.*, 109:263001, 2012.
- [28] Yu-Ping Sun, Ji-Cai Liu, Chuan-Kui Wang, and Faris Gel'mukhanov. Propagation of a strong x-ray pulse: pulse compression, stimulated raman scattering, amplified spontaneous emission, lasing without inversion, and four-wave mixing. *Phys. Rev. A*, 81:013812, 2010.
- [29] F. Bencivenga, R. Cucini, F. Capotondi, A. Battistoni, R. Mincigrucci, E. Giangrisostomi, A. Gessini, M. Manfredda, I. P. Nikolov, E. Pedersoli, E. Principi, C. Svetina, P. Parisse, F. Casolari, M. B. Danailov, M. Kiskinova, and C. Masciovecchio. Four-wave mixing experiments with extreme ultraviolet transient gratings. *Nature*, 520:205–208, 2015.
- [30] Ji-Cai Liu, Yu-Ping Sun, Chuan-Kui Wang, Hans Ågren, and Faris Gel'mukhanov. Auger effect in the presence of strong x-ray pulses. *Phys. Rev. A*, 81:043412, 2010.
- [31] Philipp V. Demekhin and Lorenz S. Cederbaum. Strong interference effects in the resonant Auger decay of atoms induced by intense x-ray fields. *Phys. Rev. A*, 83:023422, 2011.
- [32] Christian Buth and Kenneth J. Schafer. Ramsey method for Auger-electron interference induced by an attosecond twin pulse. *Phys. Rev. A*, 91:023419, Feb 2015.
- [33] Bob Nagler, Ulf Zastra, Roland R. Fäustlin, Sam M. Vinko, Thomas Whitcher, A. J. Nelson, Ryszard Sobierajski, Jacek Krzywinski, Jaromir Chalupsky, Elsa Abreu, Saša Bajt, Thomas Bornath, Tomas Burian, Henry Chapman, Jaroslav Cihelka, Tilo Döppner, Stefan Düsterer, Thomas Dzelzainis, Marta Fajardo, Eckhart Förster, Carsten Fortmann, Eric Galtier, Siegfried H. Glenzer, Sebastian Göde, Gianluca Gregori, Vera Hajkova, Phil Heimann, Libor Juha, Marek Jurek, Fida Y. Khattak, Ali Reza Khorsand, Dorota Klinger, Michaela Kozlova, Tim Laarmann, Hae Ja Lee, Richard W. Lee, Karl-Heinz Meiwes-Broer, Pascal Mercere, William J. Murphy, Andreas Przystawik, Ronald Redmer, Heidi Reinholz, David Riley, Gerd Röpke, Frank Rosmej, Karel Saksl, Romain Schott, Robert Thiele, Sven Tiggesbäumker, Josef Toleikis, Thomas Tschentscher, Ingo Uschmann, Hubert J. Vollmer, and Justin S. Wark. Turning solid aluminium transparent by intense soft x-ray photoionization. *Nature Phys.*, 5:693–696, 2009.
- [34] Christian Buth, Ji-Cai Liu, Mau Hsiung Chen, James P. Cryan, Li Fang, James M. Glowina, Matthias Hoener, Ryan N. Coffee, and Nora Berrah. Ultrafast absorption of intense x rays by nitrogen molecules. *J. Chem. Phys.*, 136:214310, 2012.
- [35] N. Gerken, S. Klumpp, A. A. Sorokin, K. Tiedtke, M. Richter, V. Bürk, K. Mertens, P. Juranić, and M. Martins. Time-dependent multiphoton ionization of xenon in the soft-x-ray regime. *Phys. Rev. Lett.*, 112:213002, 2014.
- [36] Richard Neutze, Remco Wouts, David van der Spoel, Edgar Weckert, and Janos Hajdu. Potential for biomolecular imaging with femtosecond x-ray pulses. *Nature*, 406:752–757, 2000.
- [37] Gábor Darvasi, Christoph H. Keitel, and Christian Buth. Optical control of an atomic inner-shell x-ray laser. *Phys. Rev. A*, 89:013823, 2014.
- [38] Christian Buth, Markus C. Kohler, Joachim Ullrich, and Christoph H. Keitel. High-order harmonic generation enhanced by XUV light. *Opt. Lett.*, 36:3530–3532, 2011.
- [39] Markus C. Kohler, Carsten Müller, Christian Buth, Alexander B. Voitkiv, Karen Z. Hatsagortsyan, Joachim Ullrich, Thomas Pfeifer, and Christoph H. Keitel. Electron correlation and interference effects in strong-field processes. In Kaoru Yamanouchi and Katsumi Midorikawa, editors, *Multiphoton Processes and Attosecond Physics*, volume 125 of *Springer Proceedings in Physics*, pages 209–217, Berlin, Heidelberg, 2012. Springer.
- [40] Christian Buth, Feng He, Joachim Ullrich, Christoph H. Keitel, and Karen Zaveni Hatsagortsyan. Attosecond pulses at kiloelectronvolt photon energies from high-order harmonic generation with

- core electrons. *Phys. Rev. A*, 88:033848, 2013.
- [41] Christian Buth. High-order harmonic generation with resonant core excitation by ultraintense x rays. *Eur. Phys. J. D*, 69:234, 2015.
- [42] Stefano M. Cavaletto, Zoltán Harman, Christian Buth, and Christoph H. Keitel. X-ray frequency combs from optically controlled resonance fluorescence. *Phys. Rev. A*, 88:063402, 2013.
- [43] Stefano M. Cavaletto, Zoltán Harman, Christian Ott, Christian Buth, Thomas Pfeifer, and Christoph H. Keitel. Broadband high-resolution x-ray frequency combs. *Nature Photon.*, 8:520–523, 2014.
- [44] A. A. Sorokin, S. V. Bobashev, T. Feigl, K. Tiedtke, H. Wabnitz, and M. Richter. Photoelectric effect at ultrahigh intensities. *Phys. Rev. Lett.*, 99:213002, 2007.
- [45] M. G. Makris, P. Lambropoulos, and A. Mihelič. Theory of multiphoton multielectron ionization of xenon under strong 93-eV radiation. *Phys. Rev. Lett.*, 102:033002, 2009.
- [46] Nina Rohringer and Robin Santra. X-ray nonlinear optical processes using a self-amplified spontaneous emission free-electron laser. *Phys. Rev. A*, 76:033416, 2007.
- [47] James P. Cryan, James M. Glowonia, J. Andreasson, Ali Belkacem, Nora Berrah, C. I. Blaga, C. Bostedt, J. Bozek, N. A. Cherepkov, L. F. DiMauro, Li Fang, O. Gessner, M. Gühr, J. Hajdu, M. P. Hertlein, M. Hoener, O. Kornilov, J. P. Marangos, A. M. March, B. K. McFarland, H. Merdji, M. Messerschmidt, V. S. Petrović, C. Raman, D. Ray, D. A. Reis, S. K. Semenov, M. Trigo, J. L. White, W. White, L. Young, P. H. Bucksbaum, and R. N. Coffee. Molecular frame Auger electron energy spectrum from N<sub>2</sub>. *J. Phys. B*, 45:055601, 2012.
- [48] A. A. Sorokin, S. V. Bobashev, K. Tiedtke, and M. Richter. Multi-photon ionization of molecular nitrogen by femtosecond soft x-ray FEL pulses. *J. Phys. B*, 39:L299–L304, 2006.
- [49] Takahiro Sato, Tomoya Okino, Kaoru Yamanouchi, Akira Yagishita, Fumihiko Kannari, Koichi Yamakawa, Katsumi Midorikawa, Hidetoshi Nakano, Makina Yabashi, Mitsuru Nagasono, and Tetsuya Ishikawa. Dissociative two-photon ionization of N<sub>2</sub> in extreme ultraviolet by intense self-amplified spontaneous emission free electron laser light. *Appl. Phys. Lett.*, 92:154103, 2008.
- [50] Y. H. Jiang, A. Rudenko, M. Kurka, K. U. Kühnel, Th. Ergler, L. Foucar, M. Schöffler, S. Schössler, T. Havermeier, M. Smolarski, K. Cole, R. Dörner, S. Düsterer, R. Treusch, M. Gensch, C. D. Schröter, R. Moshhammer, and J. Ullrich. Few-photon multiple ionization of N<sub>2</sub> by extreme ultraviolet free-electron laser radiation. *Phys. Rev. Lett.*, 102:123002, 2009.
- [51] Motomichi Tashiro, Masahiro Ehara, Hironobu Fukuzawa, Kiyoshi Ueda, Christian Buth, Nikolai V. Kryzhevoi, and Lorenz S. Cederbaum. Molecular double core-hole electron spectroscopy for chemical analysis. *J. Chem. Phys.*, 132:184302, 2010.
- [52] Nora Berrah, Li Fang, Brendan Murphy, Timur Osipov, Kiyoshi Ueda, Edwin Kukk, Raimund Feifel, Peter van der Meulen, Peter Salen, Henning T. Schmidt, Richard D. Thomas, Mats Larsson, Robert Richter, Kevin C. Prince, John D. Bozek, Christoph Bostedt, Shin-ichi Wada, Maria N. Piancastelli, Motomichi Tashiro, and Masahiro Ehara. Double-core-hole spectroscopy for chemical analysis with an intense x-ray femtosecond laser. *Proc. Natl. Acad. Sci. U.S.A.*, 108:16912–16915, 2011.
- [53] T. Y. Osipov, L. Fang, B. F. Murphy, M. Hoener, and N. Berrah. X-ray FEL induced double core-hole and high charge state production. *J. Phys.: Conf. Ser.*, 388:012030, 2012.
- [54] See the Supplementary Data for *Mathematica* [55] files for the molecular rate equation model and all computations presented in this work.
- [55] Wolfram Research, Inc., 100 Trade Center Drive, Champaign, Illinois 61820, USA. *Mathematica 10.1*, 2015.
- [56] D. R. Hartree. The wave mechanics of an atom with a non-coulomb central field. Part I. Theory and methods. *Proc. Camb. Phil. Soc.*, 24:89–110, 1928.
- [57] Attila Szabo and Neil S. Ostlund. *Modern Quantum Chemistry: Introduction to Advanced Electronic Structure Theory*. McGraw-Hill, New York, 1st, revised edition, 1989.
- [58] Kai Siegbahn, C. Nordling, G. Johansson, J. Hedman, P. F. Hedén, K. Hamrin, U. Gelius, T. Bergmark, L. O. Werme, R. Manne, and Y. Baer. *ESCA Applied to Free Molecules*. North-

- Holland, American Elsevier, Amsterdam, London, New York, 1969.
- [59] D. Stalherm, B. Cleff, H. Hillig, and W. Mehlorn. Energies of excited states of doubly ionized molecules by means of Auger electron spectroscopy. Part I. Electronic states of  $N_2^{2+}$ . *Z. Naturforsch. Teil A*, 24:1728–1733, 1969.
- [60] W. E. Moddeman, Thomas A. Carlson, Manfred O. Krause, B. P. Pullen, W. E. Bull, and G. K. Schweitzer. Determination of the  $K$ - $LL$  Auger spectra of  $N_2$ ,  $O_2$ ,  $CO$ ,  $NO$ ,  $H_2O$ , and  $CO_2$ . *J. Chem. Phys.*, 55:2317–2336, 1971.
- [61] W. C. Stolte, Z. X. He, J. N. Cutler, Y. Lu, and J. A. R. Samson. Dissociative photoionization cross sections of  $N_2$  and  $O_2$  from 100 to 800 eV. *At. Data Nucl. Data Tables*, 69:171–179, 1998.
- [62] R. W. Wetmore and R. K. Boyd. Theoretical investigation of the dication of molecular nitrogen. *J. Phys. Chem.*, 90:5540–5551, 1986.
- [63] C. Beylerian and C. Cornaggia. Coulomb explosion imaging of fragmentation channels following laser-induced double ionization of  $N_2$ . *J. Phys. B*, 37:L259–L265, 2004.
- [64] K. Codling, C. Cornaggia, L. J. Frasinski, P. A. Hatherly, J. Morellec, and D. Normand. Charge-symmetric fragmentation of diatomic molecules in intense picosecond laser fields. *J. Phys. B*, 24:L593–L597, 1991.
- [65] E. Baldit, S. Saugout, and C. Cornaggia. Coulomb explosion of  $N_2$  using intense 10- and 40-fs laser pulses. *Phys. Rev. A*, 71:021403, 2005.
- [66] Simona Scheit, Lorenz S. Cederbaum, and Christian Buth. Nonlinearity theorem of multiphoton absorption. *in preparation*, 2016.
- [67] Teijo Åberg. Two-photon emission, the radiative Auger effect, and the double Auger process. In Bernd Crasemann, editor, *Ionization and Transition Probabilities*, volume 1 of *Atomic Inner-Shell Processes*, pages 353–375, New York, 1975. Academic Press.
- [68] André D. Bandrauk, Djameladdin G. Musaev, and Keiji Morokuma. Electronic states of the triply charged molecular ion  $N_2^{3+}$  and laser-induced Coulomb explosion. *Phys. Rev. A*, 59:4309–4315, 1999.
- [69] Jens Als-Nielsen and Des McMorrow. *Elements of Modern X-Ray Physics*. John Wiley & Sons, New York, 2001.
- [70] S. Düsterer, P. Radcliffe, C. Bostedt, J. Bozek, A. L. Cavalieri, R. Coffee, J. T. Costello, D. Cubaynes, L. F. DiMauro, Y. Ding, G. Doumy, F. Grüner, W. Helml, W. Schweinberger, R. Kienberger, A. R. Maier, M. Messerschmidt, V. Richardson, C. Roedig, T. Tschentscher, and M. Meyer. Femtosecond x-ray pulse length characterization at the Linac Coherent Light Source free-electron laser. *New J. Phys.*, 13:093024, 2011.
- [71] Christian Buth, Robin Santra, and Lorenz S. Cederbaum. Impact of interatomic electronic decay processes on the width of the  $Xe 4d$  lines in the Auger decay of the xenon fluorides. *J. Chem. Phys.*, 119:10575–10584, 2003.